X-922-74-235
PREPRINT

NASA TM X- 70752

A COMPARISON OF ELECTRIC AND MAGNETIC FIELD DATA FROM THE OGO-6 SPACECRAFT

R. A. LANGEL

(NASA-TM-X-70752) A COMPARISON OF ELECTRIC AND MAGNETIC FIELD DATA FROM THE OGO-6 SPACECRAFT (NASA) 34 p HC $4.75 CSCL 03B

N74-34261

Unclas
G3/29 50110

AUGUST 1974

GODDARD SPACE FLIGHT CENTER
GREENBELT, MARYLAND

X-922-74-235

A COMPARISON OF ELECTRIC AND MAGNETIC FIELD DATA FROM THE OGO-6 SPACECRAFT

R. A. Langel
Geophysics Branch

GODDARD SPACE FLIGHT CENTER
Greenbelt, Md. 20771

A COMPARISON OF ELECTRIC AND MAGNETIC FIELD DATA FROM THE OGO-6 SPACECRAFT

R. A. Langel

Geophysics Branch
Goddard Space Flight Center
Greenbelt, Maryland 20771

ABSTRACT

Previous studies of the OGO-6 electric field data by Heppner and of magnetic field magnitude observations by Langel have indicated a distinct dependence of disturbance characteristics on interplanetary sector polarity. Examination of simultaneous patterns of disturbance below 600 km over the summer polar cap shows that pattern changes in electric field and in the disturbance in magnetic field magnitude are highly correlated. This correlation extends to pattern shapes, boundary locations, and to the amplitudes of the correlated quantities. In the winter hemisphere, at altitudes above 800 km, correlations between boundaries exist, pattern correlations are present but are not as strong as at low altitudes in summer, and amplitude correlations are essentially absent. These studies verify that below 600 km the region of positive ΔB, from 2200 to 1000 MLT, has a significant contribution from both ionospheric and non-ionospheric sources. Above 800 km the non-ionospheric sources dominate. These data also are consistent with the existence of a latitudinally broad current system at sunlit MLT as the source of the negative ΔB region between 1000 and 2200 MLT. In this region broad structures in electric field patterns and in ΔB patterns are highly correlated. Multiple peaks in the negative ΔB, presumably to be identified with the multiple peaks in negative ΔZ found by Langel (1973) in average surface data, occur when the electric field pattern has multiple reversals near dusk. Pattern variability is large enough so that it is probably not meaningful to draw equivalent current systems.

CONTENTS

LIST OF ILLUSTRATIONS

A COMPARISON OF ELECTRIC AND MAGNETIC FIELD DATA FROM THE OGO-6 SPACECRAFT

Magnetospheric and ionospheric currents causing magnetic field variations at high latitudes near the earth have principally been studied utilizing data from magnetometers at the earth's surface (see review by Rostoker, 1972). In recent years the scope of investigation has been broadened by measurements of electric field (see review by Maynard, 1972), by satellite measurements of magnetic field disturbances caused by field aligned currents (Zmuda et al., 1966, 1967; Armstrong and Zmuda, 1970, 1973; Theile and Praetorius, 1973), and by satellite measurement of disturbances in magnetic field magnitude (Dolginov et al., 1972; Langel, 1974a, 1974b). This paper utilizes simultaneous measurements of electric field (one horizontal axis only) and magnetic field (magnitude only) to further investigate the sources of disturbance in high latitude magnetic fields. The basic approach is to note the correlations in boundaries, amplitudes and other features between electric field patterns and magnetic disturbance patterns. These correlations are interpreted in terms of current locations and directions compatible with the measured electric and magnetic fields and in terms of source characteristics known from previous investigations.

The basic morphology of the variation or disturbance in total magnetic field at the POGO (OGO 2, 4, and 6) satellites, without regard to the interplanetary

magnetic field sector, and the interpretation of that morphology in terms of sources have been previously presented by Langel (1974a, b, henceforth referred to as papers I and II). A description of the dependence of this disturbance on interplanetary magnetic sector structure is given by Langel (1974c). Only the total field is measured in these experiments, and the quantity analyzed is $\Delta B = |\vec{B}| - |\vec{M}|$ where $|\vec{B}|$ (= B) is the quantity measured, and $\vec{M}$ is the corresponding field vector derived from a model of the quiet time field, represented by spherical harmonics (details are in paper I). The measurement accuracy, including orbital errors, is in general better than 6γ. Paper I describes the contours of average ΔB as a function of season, Kp, and altitude. Figure 1 illustrates the basic pattern of ΔB, which is positive from about 22^h to 10^h MLT (magnetic local time) and negative from about 10^h to 20^h MLT. The standard error of the averages from which Figure 1 is derived are $\leq 10\gamma$. This pattern is found at all seasons, Kp levels and altitudes, and its main features are two regions, denoted as the positive ΔB region and the negative ΔB region respectively. In paper II it was shown that in neither region can a latitudinally narrow electrojet current be considered as the principal source. Figure 2 summarizes the proposed source current distribution for summer months, omitting continuity in some regions where it is believed that field aligned currents may be important because conductivity gradients there are expected to exceed electric field gradients (see, e. g., Heppner, et al., 1971). A latitudinally broad current in the sunlit region between about 10^h and 19^h or 20^h MLT produces both the negative ΔB region

and positive bays in the auroral belt. The latitudinally narrow westward electrojet from about 22^h to 8^h contributes some of the positive ΔB, particularly at low altitude, but most of the positive ΔB is shown to be extra-ionospheric in origin. The latitudinally narrow eastward electrojet is only detected in low altitude passes between 18^h and 22^h MLT.

Variations in average ΔB between sectors are large in summer and small in winter. In summer, for example, in Figure 1 for away sectors the negative ΔB region extends to 8^h at 80°, while for toward sectors it extends only to about 11^h. Near $7\text{-}8^h$ above 80° for away sectors ΔB is negative ($\leq -20\gamma$ in summer), while for toward sectors ΔB is positive ($\geq 20\gamma$ in summer). The largest change occurs in the region between 80° and 86° and between $7\text{-}10^h$, where the difference in average ΔB in summer reaches 100γ. At equinox the differences in average ΔB in this region are near 20γ, while in winter, differences between the two sectors from 6^h to 18^h are of the order of the standard errors of the averages. (Season, for the average data, is defined relative to the dipole latitude of the sub-solar point, θ_{sun}, as follows: $|\theta_{sun}| < 10°$ is equinox, $\theta_{sun} > 10°$ is (northern) summer, and $\theta_{sun} < -10°$ is (northern) winter.)

It is now apparent that convective electric fields are always present over a large area of the polar regions (Heppner, 1972 a, b, c). Heppner (1972a) has succeeded in classifying the electric field distributions from OGO 6 data in terms of characteristic "signatures" in the polar-cap portion of the electric field pattern. Only passes crossing the noon-midnight meridian between Λ (invariant

latitude) = 75° on the night side and $\Lambda = 85°$ on the day side were so classified in the northern hemisphere. In the southern hemisphere, passes crossing between $\Lambda = 85°$ on the day side and $\Lambda = 85°$ on the night side were similarly classified. Using this classification in terms of signatures, Heppner was able to show a high correlation between the occurrence of away interplanetary sectors and signatures with stronger fields on the morning (evening) side of the polar cap in the northern (southern) hemisphere. During toward sectors the polar cap electric field usually was constant or had a peak in the evening in the northern hemisphere and a peak in the morning in the southern hemisphere. These correlations are illustrated in Figure 3 (From Heppner, 1972c).

Because both the average ΔB patterns and the individual electric field patterns show variations between interplanetary magnetic field sectors, it is not surprising that correlation between the characteristics of simultaneous ΔB and electric field patterns is found in the OGO-6 Data. That such correlations exist was first pointed out to the author by Heppner (personal communication, 1974).

SIGNATURE CORRELATION

Simultaneous data of good quality are available for the period 10-20 June 1969. In correlating ΔB and electric field patterns, only passes which crossed the noon-midnight meridian at $\Lambda \geq 85°$ and had well defined ΔB and electric field patterns were considered. The satellite was at low altitudes (400-600 km) in the northern (summer) hemisphere and at high altitudes (800-1050 km) in the southern (winter) hemisphere.

Pattern correlations for the northern hemisphere are illustrated by a sequence of six idealized diagrams in Figure 4. Polar cap electric field profiles include those peaked in the evening (Diagram A), relatively flat profiles (Diagram B), profiles with a tendency to peak near dawn (Diagrams C and D) and profiles having a tendency to peak near dawn with multiple crossing on the evening side of the polar cap (Diagram F). The ΔB patterns exhibit two types of variation between pattern type. First, the zero crossing between the negative and positive ΔB regions tends to move progressively from near the noon-midnight meridian toward the morning auroral belt as the patterns progress from Diagram A to Diagram F. Second, the negative ΔB region varies from a smooth curve peaked near dusk (Diagrams A-C), to a broadly peaked region (Diagram D), to a flat region over a wide range of latitudes with a peak near dusk (Diagram E), and to a multiple peaked pattern (Diagram F).

Patterns with the characteristics shown in Diagrams A-B occur almost exclusively during toward interplanetary magnetic sectors while patterns with the characteristics shown in Diagrams D through F occur almost exclusively during away sectors. Most patterns like Diagram C occur during away sectors but some occur during toward sectors. This correlation is the same as those found previously for average ΔB (Langel, 1973c) and for individual electric field patterns (Heppner, 1972c).

Some of the zero crossings, peaks and boundaries are highly correlated between the two types of data. These features being correlated are labeled on

Figure 4 with the convention that roman numerals are utilized for ΔB pattern features and arabic numerals are utilized for electric field pattern features. As far as possible, correlated features on the two pattern types are designated by the same numerical value. In particular:

a) The electric field zero crossing (4) from the polar cap to the evening auroral belt is well defined for patterns A, B, C, and D. When adequate data are available, and multiple electric field crossings do not occur. (4) is generally within about 1-3° of the minimum, (IV), of ΔB, and within 1-2° when (4) is a sharp peak.

b) For some of the very broad negative ΔB patterns D, and for patterns like E, the crossing (4) occurs near the center of the negative ΔB region, even if (IV) is not at the center of the region.

c) For multiple humped negative ΔB patterns, like pattern E or F, the crossing (4) occurs between the two minima of ΔB. If the electric field has multiple crossings, the equatorward (4) crossing is at or just poleward of the equatorward ΔB minimum and the other electric field zero crossings lie between the two ΔB minima. Sometimes the poleward electric field zero crossing is very near the poleward ΔB minimum, and, in the purest examples of Pattern F, the central zero crossing occurs within 1-2° of the maximum between the two negative ΔB minima.

d) For patterns C, D, E, and F the electric field maximum near dawn, (7), almost always occurs poleward of the positive ΔB peak, generally about 2-5° poleward, and to the dawn side of the ΔB zero crossing, (VII).

e) When it is well defined, the electric field peak, (2), in the morning auroral belt occurs between the ΔB peak, (III), and zero crossing (II), i.e. on the slope between (III) and (II). Structure in this portion of the electric field usually corresponds to structure in the ΔB curve. For example, on Figure 5 near 9^h 12 min two electric field peaks occur and an inflection occurs in ΔB such that each peak in electric field occurs in a portion of ΔB with a distinct slope. (Figure 5 also serves as an example of a pattern with features like diagrams E and F of Figure 4.) Cases can also be found of electric field structure in this region with no apparent corresponding ΔB structure.

f) The electric field zero crossing, (3), and the positive ΔB peak, (III), often occur within 1-2° of each other, with some tendency for (III) to be poleward of (3).

g) The electric field peak, (5), generally occurs on the ΔB slope between (IV) and (V).

Southern hemisphere pattern correlations are not as obvious as those for the northern hemisphere. The situation is complicated by the occurrence of large fluctuations in the electric field data. Two representative passes are shown in Figure 6. As expected for high altitude (> 800 km.) winter hemisphere data (see papers I and II), the negative ΔB region is non existent or of negligible amplitude for all southern passes in this time period. The major differences in the two ΔB patterns in Figure 6 are that in Figure 6b the peak, (III), of the ΔB is more rounded (i.e. broader) and is also more poleward than the peak in

Figure 6a. Because the poleward shift of the peak, (III), in Figure 6b is greater than the accompanying poleward shift of the zero crossing (II), the morning and evening side slopes of the ΔB curve are more nearly equal in Figure 6b than in Figure 6a. In most of the southern hemisphere passes with well defined ΔB patterns the patterns are either like those in Figure 6 or have characteristics between these two extremes.

The polar cap electric field pattern in Figure 6a is relatively flat, although there is a peak on the evening side and a large peak on the morning side. A somewhat unusual feature of Figure 6b is that the auroral belt electric field on the dawn side extends to the pole. The polar cap electric field pattern in Figure 6b is peaked in the evening. In Figure 6b the polar cap electric field (i.e. the section of positive electric field) shows a tendency to be divided into two sections. The poleward section is of lower magnitude and has smaller fluctuations. At about 79° a jump in magnitude occurs and this equatorward segment, on the evening side, has a large number of high amplitude fluctuations together with a tendency for a broad peak in the pattern one would get if a smooth curve were run through the fluctuations. This double amplitude type structure occurs on several passes.

Although the correlations are not as definite as in the northern hemisphere, ΔB patterns similar to Figure 6a tend to be associated with relatively flat electric field patterns with a tendency to peak in the morning, and with electric field patterns with a definite peak in the morning. ΔB patterns similar to Figure 6b

tend to be associated with polar cap electric field patterns peaked in the evening. With respect to interplanetary magnetic sectors, patterns like Figure 6a tend to occur during toward sectors and patterns like Figure 6b tend to occur during away sectors. The percentage of exceptions to these trends is significantly higher in the southern hemisphere than the percentage of exceptions to the correlations discussed for the northern hemisphere data.

Figure 7 illustrates another type of ΔB pattern which occurs in the southern hemipshere. In these cases the magnitude of the positive ΔB remains high over a larger portion of the orbit, resulting in patterns with more of a "flat" type distribution than seen in Figure 6. This type of pattern is relatively rare in the time period under consideration but is common in some other time periods. Because of the sparcity of cases, it is not possible to establish a good correlation with either the electric field patterns or with interplanetary magnetic sectors. Both polar cap electric field patterns shown are relatively flat; the interplanetary field is away for Figure 7a and toward for Figure 7b.

Southern hemisphere correlations between peaks and zero crossings are as follows (see, e. g., Figure 6):

a) As in the northern hemisphere, the electric field peak, (2), in the morning auroral belt occurs between the ΔB peak, (III), and zero crossing, (II), i.e. on the slope between (II) and (III). Unlike the northern hemisphere, structure in this portion of the electric field is not found to correspond to structure in the ΔB curve.

b) In most cases the electric field crossing (3) is not well defined because large fluctuations result in multiple crossings. When defined single crossings do occur, (3) is usually within 2° of the ΔB peak (III). When the ΔB pattern is of the type illustrated in Figure 6a, the multiple electric field zero crossings occur both equatorward and poleward of the ΔB peak (III). When the ΔB pattern is of the type illustrated in Figure 6b, the multiple electric field zero crossings tend to occur poleward of (III).

c) The evening auroral belt segment of the electric field is always equatorward of the main portion of positive ΔB. When the ΔB zero crossing (VIII) is well defined, as in Figure 6a, the auroral portion of the electric field is equatorward of (VIII).

In addition to the patterns shown in Figures 4-7 are some patterns observed only during very quiet magnetospheric conditions. In the northern hemisphere, quiet time patterns sometimes have the form shown in Figure 8. Both the ΔB and the electric field are of low magnitude and both have a sinusoidal appearance. Because of uncertainties in both the magnetic field data and in the spherical harmonic model used to compute ΔB, the ΔB zero level is uncertain to about 5-10γ. The nature of the ΔB, i.e. its sinusoidal character and the locations of the ΔB peaks, does not change significantly between field models, but the locations of the zero crossings of ΔB are uncertain. Comparison of Figure 8 with pattern F of Figure 4 (note that positive values are up on Figure 4 but down on Figure 8) indicates that the patterns of Figure 8 may be an extreme form of pattern F of

Figure 4. Examination of Figure 8 shows a tendency for zero crossings of the electric field to occur at or near peak values of ΔB. Perhaps the most puzzling feature is the continuation of the sinusoidal ΔB variations to lower latitudes than the electric field oscillations in Figure 8b. In the absence of this feature it would be possible to account for the ΔB pattern in terms of Hall currents in the directions implied by the electric field.

Heppner (1973) has noted a tendency for weak electric fields in the northern hemisphere to occur on the same orbit as highly irregular electric fields in the southern hemisphere. These are, of course, also very quiet periods in terms of magnetic activity. The southern ΔB during these passes shows very little variation but often has a positive value between 5-15 γ. The reason for this positive ΔB is uncertain. Possibilities include: 1) a field due to a lithospheric magnetic anomaly not completely described by the field models used, 2) incomplete representation of fields from the equatorial current sheet by the field models used, 3) inadequate knowledge of the spacecraft orbit, or 4) fields from an ionospheric source. Because of the highly irregular nature of the electric fields, possibility 4) seems unlikely. The other possibilities are under investigation.

AMPLITUDE CORRELATIONS

Amplitude correlations are difficult to make in a clearly meaningful way. It is possible to compare either the peak of the electric field or the potential drop over the polar cap with ΔB. Examination of the individual passes indicates

a general tendency for large values of ΔB to be associated with higher values of electric field.

The following procedure has been followed to make a semi-quantitative comparison of ΔB and electric field amplitudes:

1) an "average" magnitude for the polar cap electric field is estimated.
2) The satellite path length, in units of 10° dipole latitude, is estimated for that portion of the pass when polar cap type electric fields are present.
3) The product of the above two quantities, called Me, is used to estimate the "strength" of the potential drop.
4) Me is then plotted versus the peak value of positive and negative ΔB.

The results for northern hemisphere negatives ΔB are given in Figure 9. Because of the uncertainty in finding the average value of electric field, widely varying types of electric field patterns were initially plotted with different symbols. However, no significant differences were noticeable so this practice was discontinued. A definite trend of increasing ΔB with increasing Me is seen in Figure 9, but the scatter is large.

A similar but weaker, trend is found for positive ΔB in the northern hemisphere at the southern hemisphere positive ΔB shows no definite trend as a function of Me. Correlation coefficients between ΔB and Me are 0.58, 0.49, and 0.36 for the northern hemisphere negative ΔB, the northern hemisphere positive ΔB, and the southern hemisphere positive ΔB respectively. The scatter

in the positive ΔB vs. Me comparison is not solely due to uncertainties in estimating Me. This is shown by the existence of passes on which the electric field is fairly similar both in pattern and magnitude, yet on which the positive ΔB differs by as much as a factor of two.

DISCUSSION

Langel (paper I and II) concluded that all of the negative ΔB is due to a latitudinally broad ionospheric E region current with little, if any, contribution from latitudinally narrow jet-type currents. The positive ΔB was attributed to both a westward electrojet and to a non-ionospheric source of positive ΔB. At altitudes less than 550 km these two sources were, on the average, thought to contribute nearly equally to the positive ΔB.

Consider first the negative ΔB region. If the source of ΔB were a jet-type current in the auroral belt, the maximum current would flow in the region of auroral belt electric field, i.e. near peak (5) in Figure 4, and ΔB would show a negative peak poleward and a positive peak equatorward of this current. For this case one would expect the ΔB zero crossing, (V), to be well defined and located near the electric field peak, (5). On the other hand, for a broad current of the S_q^p type, one would expect a large negative ΔB near the current vortex. Further, the current vortex would be located at the zero crossing, (4), of the electric field. The strong correlation observed between the electric field zero crossing, (4), and the peak negative ΔB, (IV), strongly supports this second interpretation.

Langel (1973) and Langel and Brown (1974) noted two distinct negative peaks in the averaged ΔZ at the earth's surface during away sectors for summer. Since $\Delta B \doteq \Delta Z$ at these latitudes, it is appropriate to look for this feature in the satellite ΔB. Such a feature is <u>not</u> apparent in the averaged ΔB (Langel, 1974c). However, the existence of field patterns such as F, and to a certain extent E, of Figure 4 and Figure 5 shows that such a feature can be present in the ΔB data, and that it is associated with structure in the electric field pattern, as would be expected if the source was an ionospheric current. From the averaged surface ΔZ it was not possible to tell if the two negative ΔZ peaks are a permanent feature during away sectors. From the present data it can be seen that this is not a permanent feature but depends upon the electric field configuration. It seems probable that the patterns of Figure 4 may be regarded as a logical sequence corresponding to the way the magnetospheric plasma flow changes in response to interplanetary conditions. The sequence of conditions is only partially known, (i. e., the response to the azimuthal component of interplanetary field).

As already noted, Figure 4 is an idealization; much more variety/variability is present in the original data. Clearly, it is not meaningful to draw equivalent current patterns to represent the observed data in any detailed fashion. The general features of the electric field and ΔB patterns do, however, support the notion of a broad S_q^p - like current in the 11-18^h MLT region, as illustrated in Figure 2, with large-variability with time. For example, the variant corresponding to pattern E of Figure 4 might be like the current sketched in Figure 10.

In the positive ΔB region the relation between the electric field peak and zero crossing, (2) and (3), and the ΔB peak, (III), is similar to the relation between the electric field peak and zero crossing, (5) and (4), and the ΔB peak, (IV), in the negative ΔB region. In contrast to the negative ΔB region, a significant number of cases exist for the positive ΔB region where a substantial negative ΔB is present equatorward of the auroral belt zero crossing of ΔB. This configuration is exactly what is expected from the combination of the westward electrojet with a non-ionospheric source. The vertical field disturbance from the non-ionospheric source reduces the magnitude of the equatorward ΔB and shifts the ΔB zero crossing equatorward. At times when the westward jet beneath the satellite is weak or absent and at high altitudes where the electrojet field is weak, the equatorward negative ΔB is small or absent.

It is of course not possible to verify the existence of a non-ionospheric positive ΔB from the northern hemisphere data alone. The electric field and ΔB patterns would also permit interpretation of the positive ΔB region in terms of a latitudinally broad ionospheric current together with a westward electrojet. The existence of the non-ionospheric positive ΔB was inferred in paper II from the altitude variation of the positive ΔB. In particular, for a fixed Kp range, the average $|\Delta B|$ decreases less than a factor of two between 450 and 1000 km in the positive ΔB region, whereas the decrease is generally greater than a factor of ten in the negative ΔB region. This altitude variation may be seen in a semi-quantitative way in the present data. The magnitude of negative ΔB at low altitudes

in the summer is comparable to the magnitude of the positive ΔB, whereas at high altitudes in the winter the negative ΔB is negligible. On the other hand, the positive ΔB at high altitudes in the winter is roughly half the magnitude of the positive ΔB at low altitudes in the summer.

The presence of some correlation in pattern features between the morning auroral belt electric field and the positive ΔB for the low altitude data is indicative of at least a partial ionospheric source. On the other hand, lack of detailed correlation is evidence that a non-ionospheric source also exists. The existence of cases where the negative ΔB equatorward of the auroral belt zero crossing of ΔB is within a factor of 3 in magnitude of the positive ΔB peak indicates that at least a portion of the ionospheric current is at times latitudinally narrow, or jet-like. However, the absence of this equatorward negative ΔB cannot be taken to indicate the absence of a jet-type current, because it is possible for a non-ionospheric positive ΔB to be large enough to completely obscure the negative ΔB in this region.

Consideration of the correlation coefficients between M_c and the peak $|\Delta B|$ also supports the proposed source distribution of Figure 2. The region of ΔB attributed mainly to ionospheric current, namely the northern hemisphere negative ΔB region, has the highest correlation coefficient, 0.58. The lowest correlation coefficient, 0.36, is obtained for the southern, higher altitude, positive ΔB region which is the region thought to be dominated by a non-ionospheric source. Lying between these two regions is the low altitude northern positive ΔB region with a

correlation coefficient of 0.49. This is the region where ΔB is thought to be due to both ionospheric and non-ionospheric sources, in about the same proportion.

It has been shown that the ΔB magnitude and electric field magnitude are not significantly correlated in the southern (winter, altitude > 800 km) data and that no correspondence between electric field fluctuations and ΔB fluctuations is found in the south, in contrast to cases like Figures 5 and 8 in the northern data. Yet the overall correlation between the dawn boundaries of the ΔB and electric field patterns is as strong in the south as it is in the north. Examination of individual passes from both hemispheres shows that this correlation occurs even when latitude shifts of 5-12° in these boundaries occur for passes at similar UT. This correlation implies that a portion of the non-ionospheric source of positive ΔB may be located at or near the equatorward convection boundary. Langel (paper II; 1974d) has already considered that the equatorial current sheet (ECS, or ring current) may be a source of high latitude positive ΔB. Examples were given in paper II of individual passes where reasonable estimates of combinations of disturbance from the ECS and electrojet sources were not consistent with the measured positive ΔB. Also, a comparison of nearly simultaneous data from COSMOS-321 at about 200 km and OGO-6 at about 800 km indicates that the positive ΔB is not caused by ionospheric currents together with the ECS unless the induced currents associated with the ECS are much smaller than is indicated by low latitude data (Langel, 1974d). From the present study there are two features of the high altitude data from the southern hemisphere which seem

inconsistent with the ECS as the major source. The disturbance due to the ECS is expected to cause a disturbance aligned according to the dipole axis. Changes in the ECS might result in magnitude changes in a ΔB pattern but should not result in the 5-12° latitude shifts that have been noted to correlate with the electric field peak (2). Also, a symmetric magnetospheric disturbance aligned according to the dipole axis should have its peak at or near the dipole pole. When assymetry exists in the ECS, the disturbance magnitude is greater in the evening than in the morning. The positive ΔB peak, however, usually occurs at least 7-10° equatorward of that pole on the morning side.

Because a non-ionospheric source is required for high latitude positive ΔB, and because the ECS does not seem capable of causing the measured disturbance, another source is required. Such a source must be consistent with the correlation between E-field and ΔB pattern boundaries. When discussing deficiencies in the ability of a model magnetospheric current system, Sugiura and Poros (1973) noted that to date such models do not include current flow in the dayside cusp. Also not included is the possibility of current flow in the high latitude "horns" of the nightside plasma sheet. Sugiura (1974) has recently shown how the magnetic field in these regions is topologically connected. It seems possible that some sort of current at relatively low altitude ($\geq$ 1000 km, say) in this region could be the source of high latitude ΔB.

ACKNOWLEDGEMENTS

I am indebted to J. P. Heppner for the use of the OGO-6 electric field data and to N. C. Maynard, J. P. Heppner, and D. P. Stern for valuable critical discussion.

REFERENCES

Armstrong, J. C., and A. J. Zmuda, Field-aligned current at 1100 km in the auroral region measured by satellite, J. Geophys. Res., 75, 7122, 1970.

Armstrong, J. C., and A. J. Zmuda, Triaxial magnetic measurements of field-aligned currents at 800 km in the auroral region: Initial results, J. Geophys. Res., 78, 6802, 1973.

Dolginov, Sh. Sh., L. N. Zhigalov, L. V. Strunnikova, Ya. I. Feldshteyn, T. N. Cherevko, and V. A. Sharova, Magnetic Storm of March 8-10, 1970, according to ground based and Kosmos-321 observations, Geomagn. i. aeronomiya, 12, Engl. trans., 909-918, 1972.

Heppner, J. P., Electric field variations during substorms; OGO 6 measurements, Planet. Space Sci., 20, 1475-1498, 1972.

Heppner, J. P., Electric fields in the magnetosphere. Critical Problems of Magnetospheric Physics, proceedings of a Joint COSPAR/IAGA/URSI Symposium, Madrid, Spain, 11-13 May 1972 (ed. E. R. Dyer), p. 107 IUCSTP Secretariat, c/o National Academy of Sciences, Washington, D. C., U.S.A., 1972b.

Heppner, J. P., Polar cap electric field distributions related to the interplanetary magnetic field direction, J. Geophys. Res., 77, 4877, 1972c.

Heppner, J. P., High latitude electric fields and the modulations related to interplanetary magnetic field parameters, Radio Science, 8, 933, 1973.

Heppner, J. P., J. D. Stolarik, and E. M. Wescott, Electric field measurements and the identification of currents causing magnetic disturbances in the polar cap, J. Geophys. Res., 76, 6028, 1971.

Langel, R. A., Average high latitude magnetic field: Variation with interplanetary sector and with season; I. Disturbed conditions, Planet. Space Sci., 21, 839, 1973.

Langel, R. A., Near earth magnetic disturbance in total field at high latitudes; I. Summary of data from OGO's 2, 4 and 6, J. Geophys. Re , 79, 2363, 1974a.

Langel, R. A., Near earth magnetic disturbance in total field at high latitudes; II. Interpretation of data from OGO's 2, 4, and 6, J Geophys. Res., 79, 2373, 1974b.

Langel, R. A., Variation with interplanetary sector of the total magnetic field measured at the OGO 2, 4, and 6 satellites, Planet. Space Sci., in Press, 1974c.

Langel, R. A., A Comparison of High latitude magnetic field data from OGO-6 and Kosmos-321; Abstract (manuscript in preparation) EOS, trans. Agu. 55, 403, 1974d.

Langel, R. A. and N. Brown, Average High Latitude magnetic field: Variations with interplanetary sector and with season, II. Comparison of disturbance levels and discussion of ionospheric currents, accepted for publication in Planet. Space Sci., 1974.

Maynard, N. C., Electric fields in the ionosphere and magnetosphere, in Magnetosphere Ionosphere interactions, ed. K. Folkestad, Universitetsforlaget, Oslo, 1972.

Rostoker, G., Polar magnetic substorms, Rev. Geophys. Space Phys., 10, 157-211, 1972.

Sugiura, M., Identification of the Polar Cap Boundary and the Auroral Belt in the High-Altitude Magnetosphere: A model for field-aligned currents, Report X-625-74-195, Goddard Space Flight Center, June 1974.

Sugiura, M. and D. J. Poros, A magnetospheric field model incorporating the OGO 3 and 5 magnetic field observations, Planet. Space Sci., 21, 1763-1773, 1973.

Theile, B., and H. M. Praetorius, Field aligned currents between 400 and 3000 km in auroral and polar latitudes, Planet. Space Sci., 21, 173, 1971.

Zmuda, A. J., F. T. Heuring, and J. H. Martin, Transverse magnetic disturbance at 1100 kilometers in the auroral region, J. Geophys. Res., 71, 5033-5045, 1966.

Zmuda, A. J., F. T. Heuring, and J. H. Martin, Day side magnetic disturbances at 1100 kilometers in the auroral oval, J. Geophys. Res., 72., 1115-1117, 1967.

CAPTIONS

Figure 1. Average ΔB (γ) from OGO 2, 4, and 6 for Kp = 2- to 3+, altitude < 550 km, and northern hemisphere. (From Langel, 1974c).

Figure 2. Conceptual drawing of proposed current sources (Langel, 1974b). The latitudinally broad current in the negative ΔB region, 11^h to 18^h MLT, is called the HLS current (High Latitude, Sunlit). Eastward and westward electrojets are shown as large arrows. These currents are assumed to flow in the ionospheric E region and this figure is for the summer season. The positive ΔB region, shaded, is due to a non-ionospheric source(s) in addition to the westward electrojet. Coordinates are invariant latitude and magnetic local time.

Figure 3. The interplanetary magnetic field ζ angle distributions for polar-cap electric field signatures. (From Heppner, 1972c).

Figure 4. Illustration of correlation between ΔB and electric field patterns in the northern (summer) hemisphere. Boundaries and zero crossings are labeled with Roman numerals for the ΔB and Arabic numerals for the electric field.

Figure 5. Example of ΔB pattern and simultaneous electric field pattern in the northern hemisphere.

Figure 6. Examples of ΔB and electric field patterns in the southern hemisphere. Coordinates are dipole latitude and magnetic local time.

Figure 7. Examples of ΔB and electric field patterns in the southern hemisphere. Coordinates are dipole latitude and magnetic local time.

Figure 8. ΔB and electric field patterns from selected quiet periods. Data are from the northern hemisphere and coordinates are dipole latitude and magnetic local time.

Figure 9. Scatter diagram of Me vs. the peak magnitude of negative ΔB in the northern hemisphere.

Figure 10. Qualitative sketch of a type of current flow consistent with multiple peaks in the negative ΔB region and with the associated electric field.

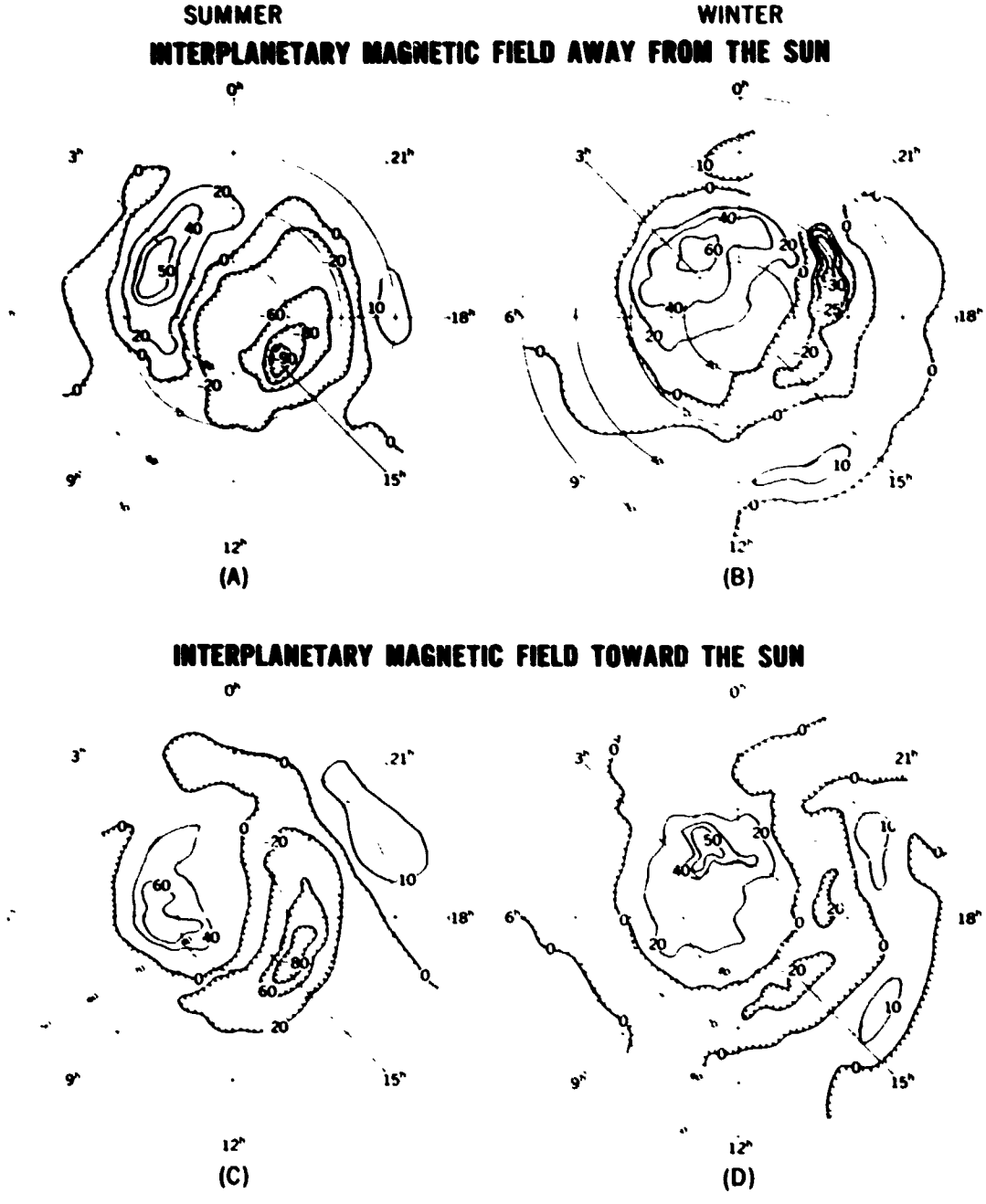

Figure 1. Average ΔB (γ) from OGO 2, 4, and 6 for Kp = 2- to 3+, altitude < 550 km, and northern hemisphere. (Fron Langel, 1974c).

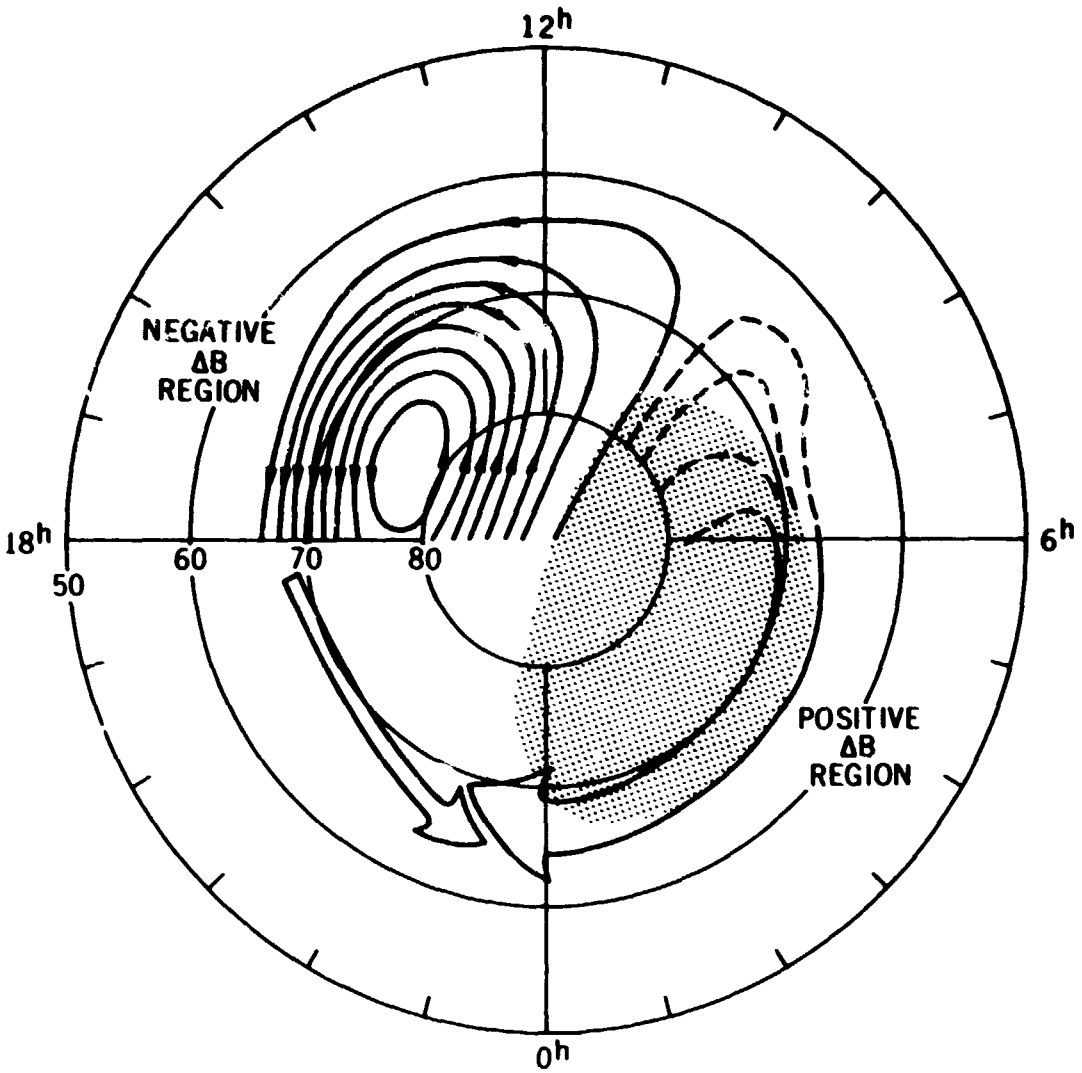

Figure 2. Conceptual drawing of proposed current sources (Langel, 1974b). The latitudinally broad current in the negative ΔB region, 11^h to 18^h MLT, is called the HLS current (High Latitude, Sunlit). Eastward and westward electrojets are shown as large arrows. These currents are assumed to flow in the ionospheric E region and this figure is for the summer season. The positive ΔB region, shaded, is due to a non-ionospheric source(s) in addition to the westward electrojet. Coordinates are invariant latitude and magnetic local time.

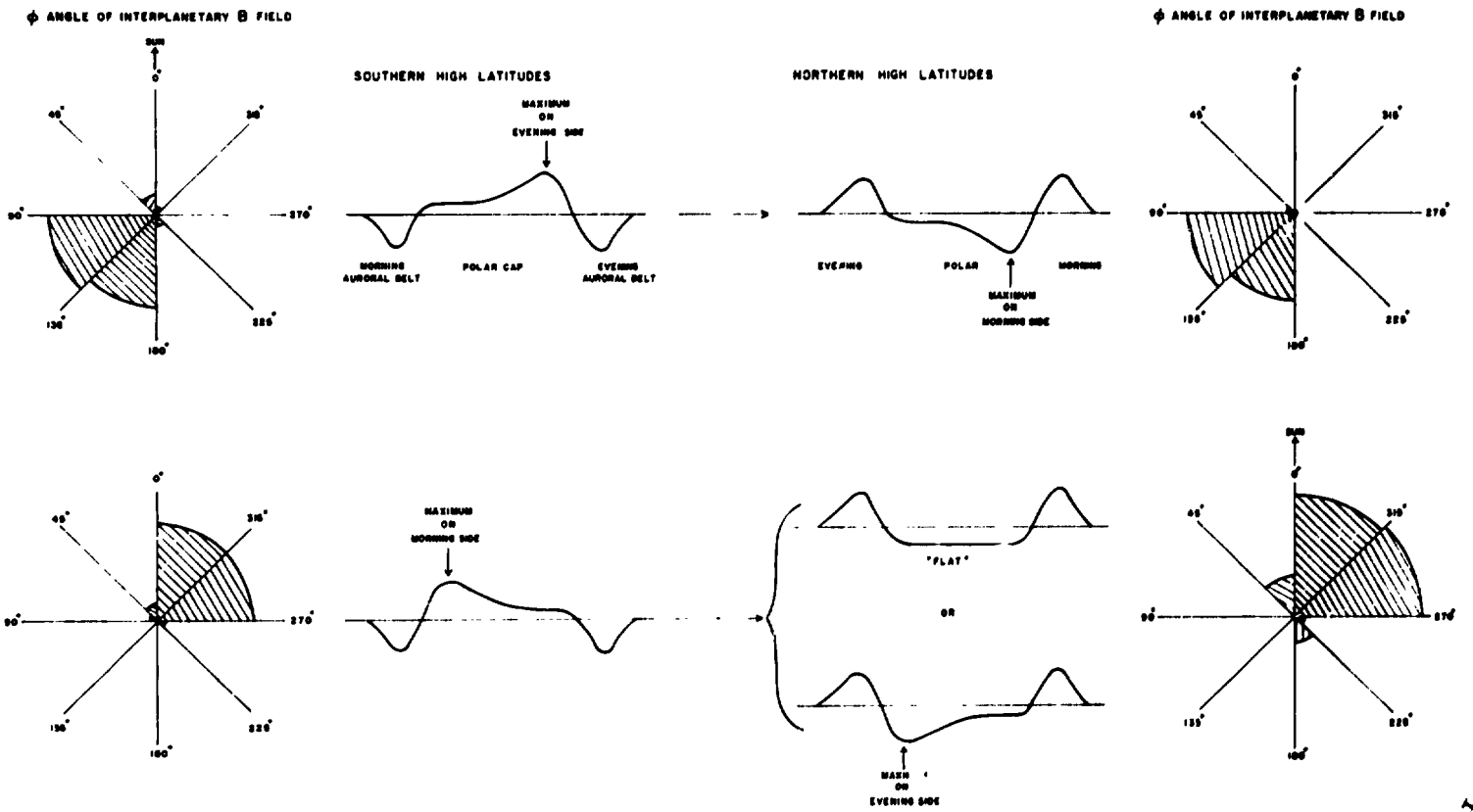

Figure 3. The interplanetary magnetic field ϕ angle distributions for polar-cap electric field signatures. (From Heppner, 1972c).

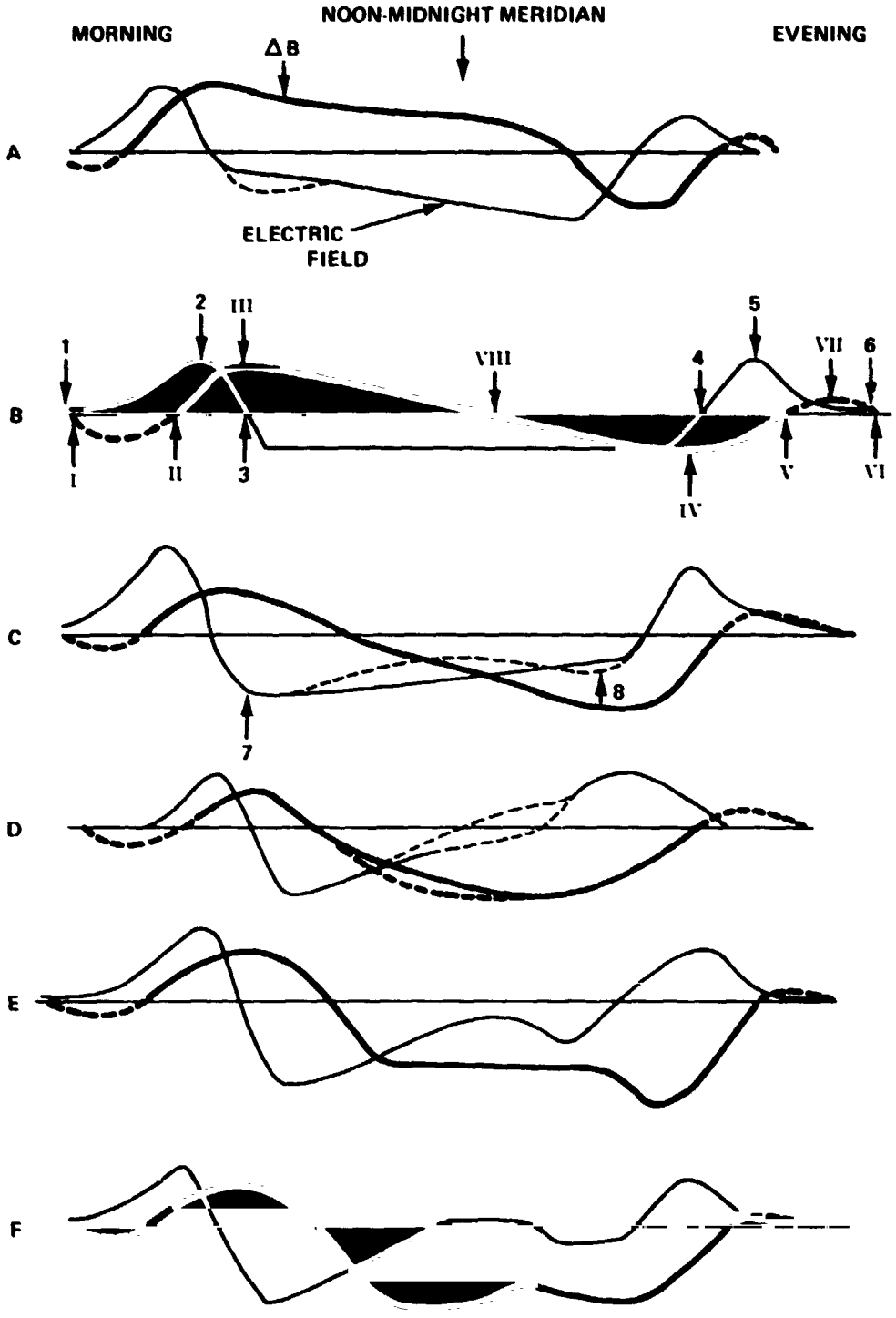

Figure 4. Illustration of correlation between ΔB and electric field patterns in the northern (summer) hemisphere. Boundaries and zero crossings are labeled with Roman numerals for the ΔB and Arabic numbers for the electric field.

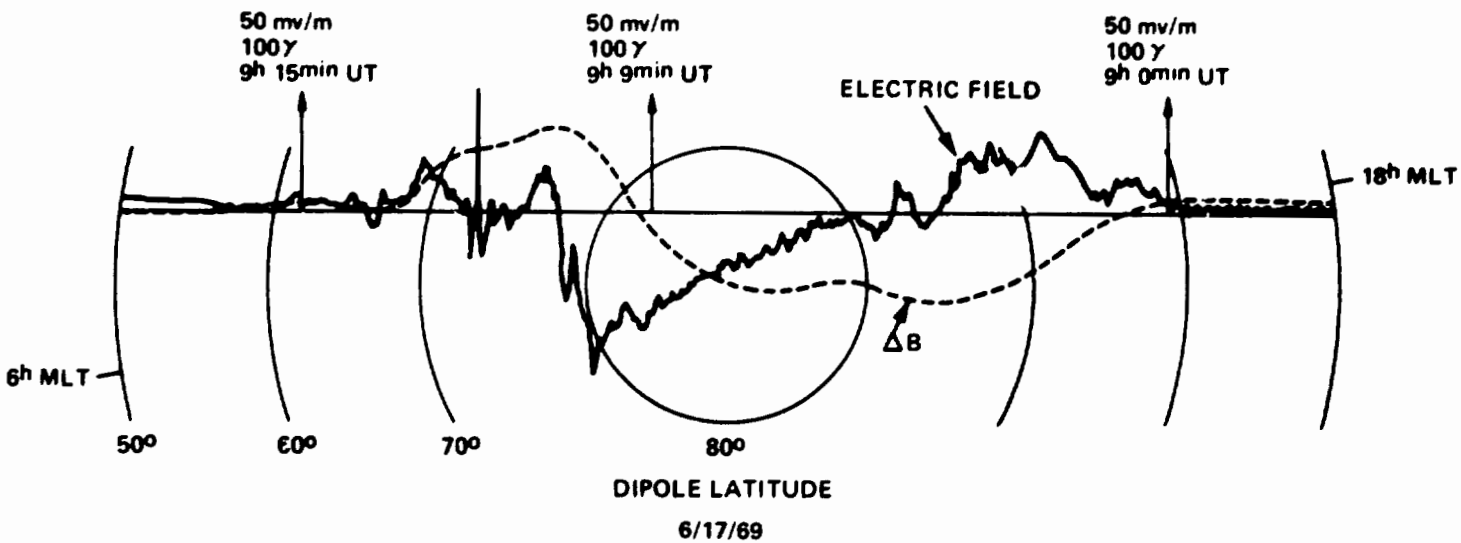

Figure 5. Example of ΔB pattern and simultaneous electric field pattern in the northern hemisphere.

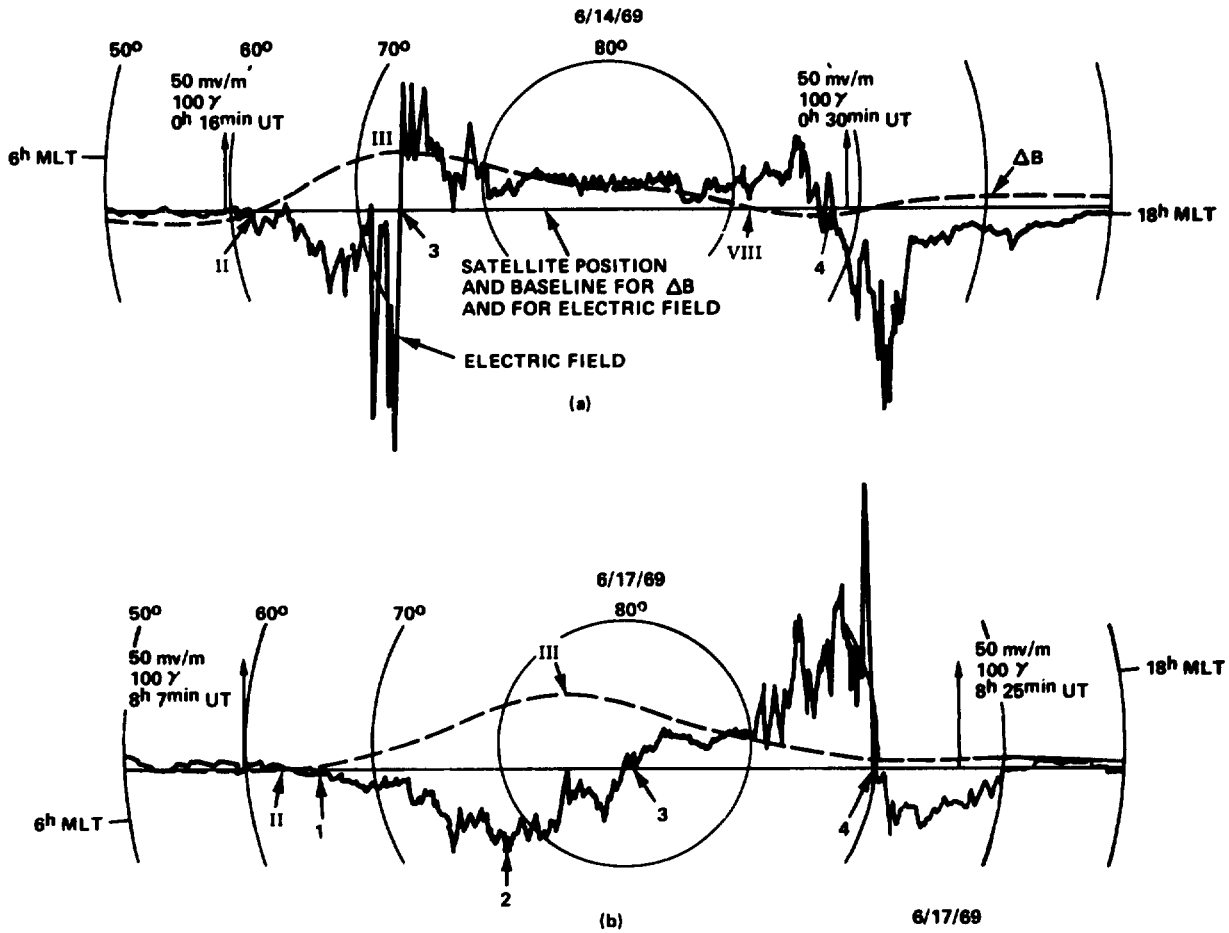

Figure 6. Examples of ΔB and electric field patterns in the southern hemisphere. Coordinates are dipole latitude and magnetic local time.

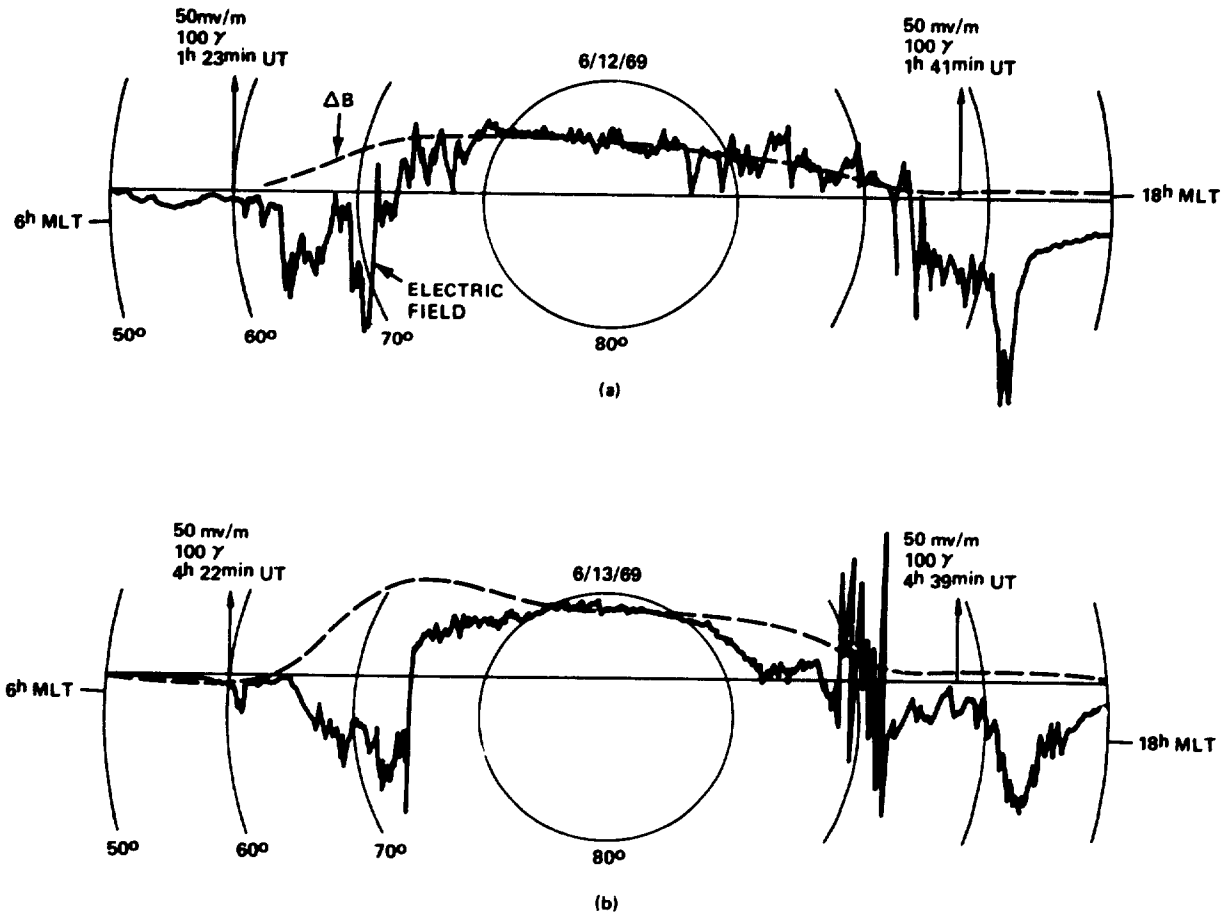

Figure 7. Examples of ΔB and electric field patterns in the southern hemisphere. Coordinates are dipole latitude and magnetic local time.

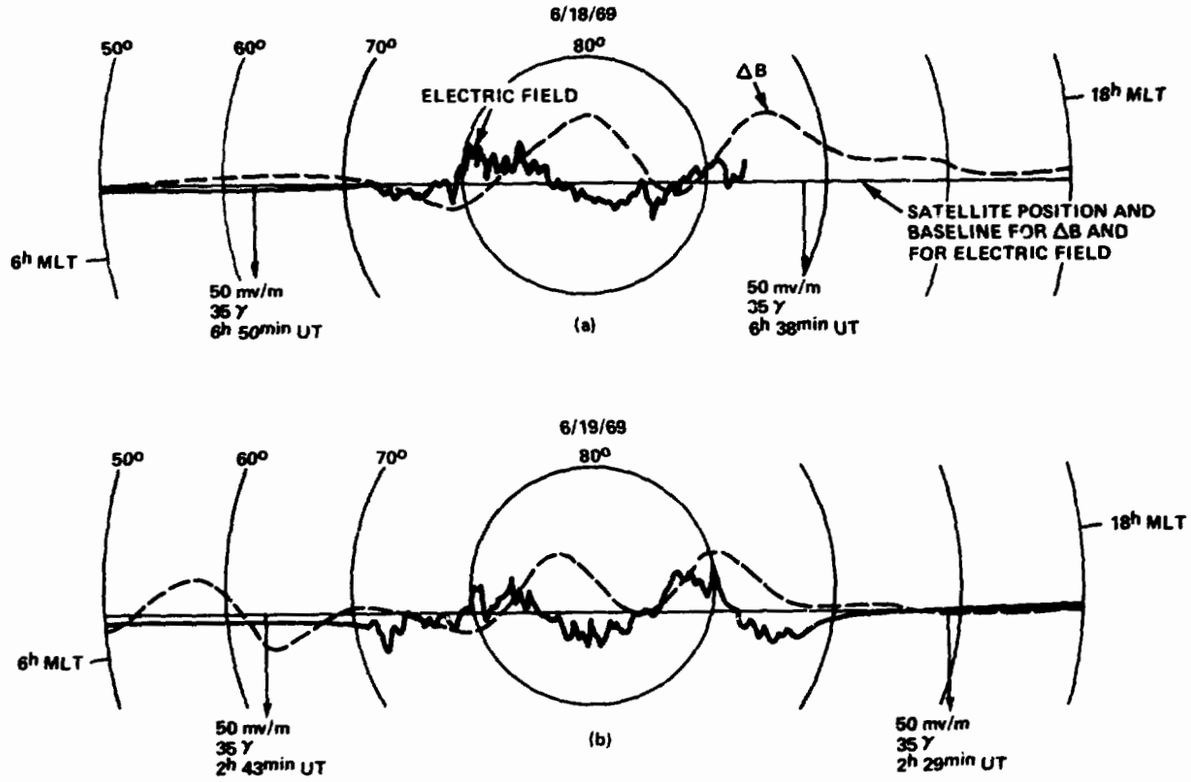

Figure 8. $\triangle$B and electric field patterns from selected quiet periods. Data are from the northern hemisphere and coordinates are dipole latitude and magnetic local time.

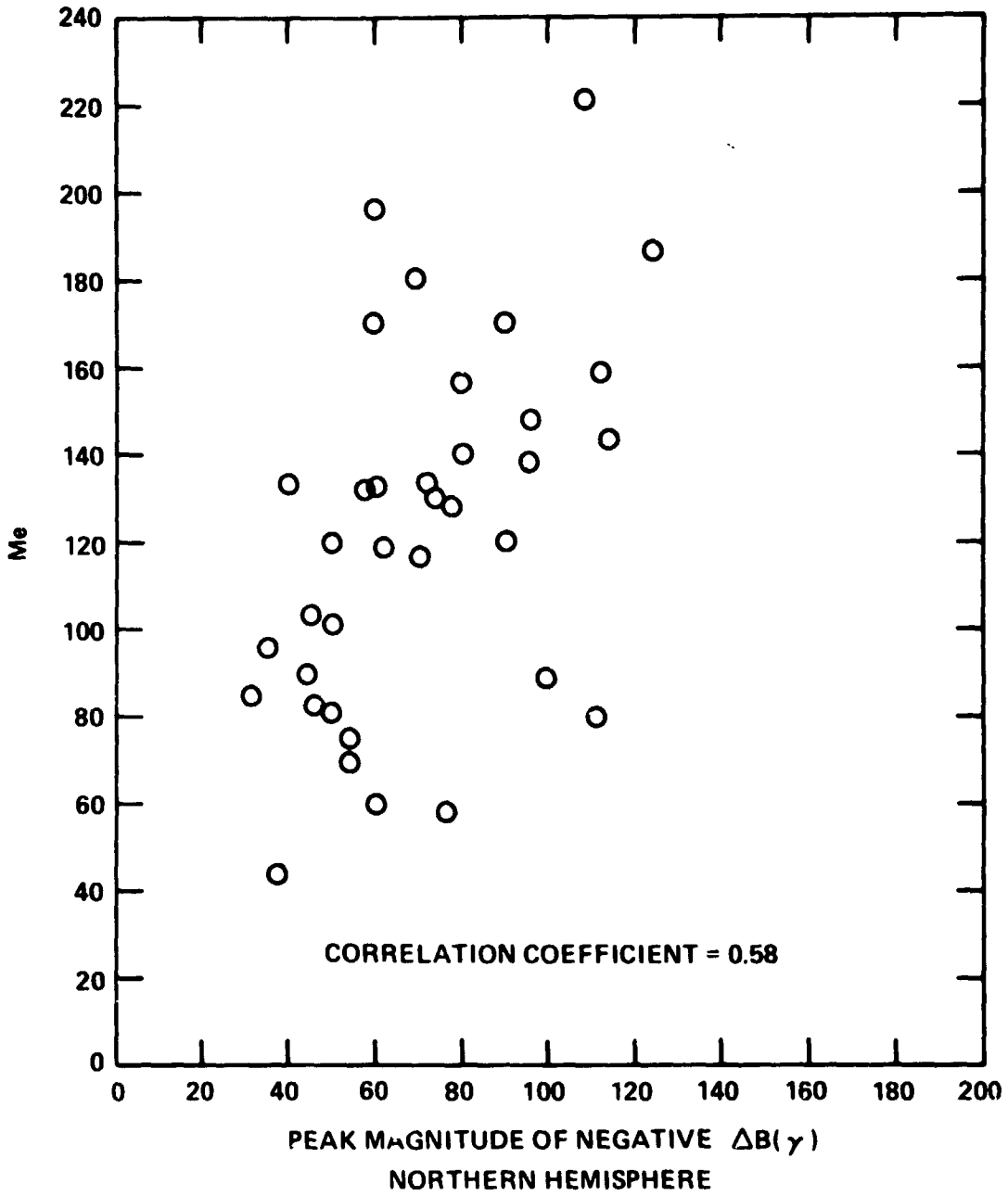

Figure 9. Scatter diagram of Me vs. the peak magnitude of negative ΔB in the northern hemisphere.